Gas-phase spectroscopic identification of the chlorovinyl radical

Carlos Cabezas, Ching-Hua Chang, Jean-Claude Guillemin, Yasuki Endo

Gas-phase spectroscopic identification of the chlorovinyl radical

Carlos Cabezas[a], Ching-Hua Chang[b], Jean-Claude Guillemin[c] and Yasuki Endo[b*]

[a] *Instituto de Física Fundamental (IFF−CSIC), Group of Molecular Astrophysics, C/ Serrano 121, 28006 Madrid, Spain*

[b] *Department of Applied Chemistry, Science Building II, National Yang Ming Chiao Tung University, 1001 Ta-Hsueh Rd., Hsinchu 300098, Taiwan*

[c] *Univ Rennes, Ecole Nationale Supérieure de Chimie de Rennes, CNRS, ISCR – UMR6226, F-35000 Rennes, France*

[*] Author to whom correspondence should be addressed. Electronic mail: endo@nycu.edu.tw

ABSTRACT

Fourier transform microwave spectra for two isomers of the chlorine substituted vinyl radical have been observed in the 4-52 GHz frequency region. The observed radicals ($^2A'$) have been generated using electric discharges of diluted dichloro derivatives of ethylene as molecular precursors. Fine and hyperfine components observed for each rotational transition are fully assigned in the present study for two isotopologues (^{35}Cl and ^{37}Cl), and precise molecular constants are determined for both radicals.

INTRODUCTION

Chlorine atoms are highly reactive and can profoundly affect atmospheric composition. It has been proposed that Cl atoms may play an important role in the chemistry of hydrocarbons in the troposphere, both in the marine boundary layer and in locations far from coastlines.[1,2] The reactions of chlorine with organic species like unsaturated hydrocarbons have received considerable interest as they are part of a fundamental class of reactions in organic chemistry, namely addition reactions.[3] The gas phase reaction of Cl atoms with unsaturated hydrocarbons proceeds via at least two competing mechanisms; addition of Cl atom to the unsaturated bond to give a chloroalkyl radical, or hydrogen abstraction to give HCl and an alkyl radical. The ratio of these two reactions has been observed to depend on hydrocarbons structure, pressure, and temperature.

The addition reaction between Cl atom and the simplest unsaturated hydrocarbon, acetylene (C_2H_2), is reported to play an important role in their removal from the marine atmosphere,[4] being also a sink of Cl atoms in the stratosphere.[5] The Cl + C_2H_2 reaction has been widely investigated both experimentally[4,6–12] and theoretically.[10,13–16] These studies indicate that two initial processes, the addition of the Cl atom to C_2H_2 to form the β-chlorovinyl radical (β-ClVR, ClHC=ĊH) and the abstraction of an H atom of C_2H_2 to form the ethynyl radical (·CCH) and HCl, are possible for this reaction. The branching ratio of these two channels depends on pressure and temperature. Quantum-chemical calculations predict that the addition reaction of Cl + C_2H_2 proceeds via a Cl-C_2H_2 pre-reactive complex to form the β-ClVR, with an exothermicity of 70-85 kJ mol^{-1}. The β-ClVR is predicted to have two isomers: *trans*-β-ClVR and *cis*-β-ClVR (see Figure 1), being the former more stable by ∼5 kJ mol^{-1} while the interconversion barrier between isomers is ∼16 kJ mol^{-1}.[14–16] In addition to the *trans* and *cis* isomers of β-ClVR, there exists another chlorovinyl radical isomer, the α-ClVR (H_2C=ĊCl), which is predicted to be ∼15 kJ mol^{-1} more stable than *trans*-β-ClVR. However, α-ClVR is not expected to be a product from the Cl + C_2H_2 reaction because its formation implies the 1,2 H atom shift whose energy barrier is very high ∼185 kJ mol^{-1}.[16]

As far as we could ascertain from the literature, the spectral identification of the ClVR isomers remains unreported in spite that the vinyl radical and its cyano-derivative have been characterized by rotational spectroscopy experiments.[17–19] In this work we present the first gas phase spectroscopic characterization of ClVR. We have employed a combination of electric discharges and Fourier transform microwave spectroscopy (FTMW) techniques to identify two isomers of ClVR in a supersonic expansion. The complex hyperfine structure of all the observed microwave transitions has been successfully assigned, and a set of precise molecular parameters including the fine and hyperfine coupling constants are experimentally determined. They are compared to those predicted by quantum chemical computations and also to those of similar molecules.

EXPERIMENTAL

The rotational spectra of the ClVR isomers were observed using a Balle-Flygare narrowband type Fourier-transform microwave (FTMW) spectrometer operating in the frequency region of 4-40 GHz.[20,21] The short-lived species α-ClVR and β-ClVR isomers were produced in a supersonic expansion by a pulsed electric discharge of a gas mixture of 1,1-dichloroethylene ($Cl_2C=CH_2$) and *trans*-1,2-dichloroethylene (HClC=CClH), respectively, diluted to 0.2% in Ar. *Trans*-1,2-dichloroethylene was obtained commercially (98%, Sigma) and used without further purification. However, since 1,1-dichloroethylene is not available in Taiwan, we sought a secure way to send this compound from France inhibiting any uncontrolled decomposition or overpressure by heating. Details are described below. The gas mixture (1,1-dichloroethylene or 1,2-dichloroethylene in Ar) was flowed through a pulsed-solenoid valve that is accommodated in the backside of one of the cavity mirrors and aligned parallel to the optical axis of the resonator. A pulse voltage of 1.3 kV with a duration of 450 μs was applied between stainless steel electrodes attached to the exit of the pulsed discharge nozzle, resulting in an electric discharge synchronized with the gas expansion. The resulting products generated in the discharge were supersonically expanded, rapidly cooled to a rotational temperature of ~2.5K between the two mirrors of the Fabry-Pérot resonator, and then probed by FTMW spectroscopy.

For measurements of the paramagnetic lines, the Earth's magnetic field was cancelled by using three sets of Helmholtz coils placed perpendicularly to one another. Since the pulsed-discharge-nozzle is arranged parallel to the cavity of the spectrometer, it is possible to suppress the Doppler broadening of the spectral lines, allowing to resolve small hyperfine splittings. The spectral resolution is 5 kHz and the frequency measurements have an estimated accuracy better than 3 kHz.

FTMW-MW double-resonance techniques[22] were employed for observing rotational transitions at frequency regions under and over 40 GHz and confirming the assignments of the transitions observed by FTMW spectroscopy. In the double-resonance experiment, a certain microwave transition was monitored by the FTMW spectrometer. Then, the intensity of the FTMW signal was recorded by scanning the frequency of the pump microwave radiation, which irradiated the discharged jet usually after the MW pulse generating the macroscopic polarization of a gas sample for FTMW spectroscopy. In this case, the macroscopic polarization is "broken" if the pump MW is resonant with a transition of which either the upper or lower level is shared by the monitored transition, so that depletion of the FTMW signal is observed.

1,1-Dichloroethylene in silica gel was shipped from France to Taiwan by standard package. Silica gel (30 g) (silica gel, pore size 60 Å, for flash chromatography, 40-63 μm particle size (RN: 112926-00-8)) was dried at 300°C under vacuum (0.1 mbar) for 3 h. After cooling to room temperature under dry nitrogen, 1,1-dichloroethylene (15 g, 0.155 mol) was added and the mixture was placed in a 50 mL flask and closed. With this 2:1 weight ratio, 1,1-dichloroethylene was stored for months and did not develop overpressure even when heated to 40°C, above its boiling point at atmospheric pressure. To collect pure 1,1-dichloroethylene, a sample was placed in a vacuum line, cooled in a liquid nitrogen bath, and evacuated. From 10 g of solid, it is thus possible to recover approximately 70% of the initial quantity of 1,1-dichloroethylene (2.3 g, 24 mmol) by heating the solid to room temperature under vacuum. A better yield (up to 80%) was obtained by heating the solid up to 80°C, but impurities were observed, although they were not a serious problem in the present study.

QUANTUM CHEMICAL CALCULATIONS

The geometry optimization calculations of ClVR ($^2A'$) were carried out using the spin-restricted coupled cluster method with single, double, and perturbative triple excitations (RCCSD(T)) and an explicitly correlated approximation (F12A)[23,24] with all electrons (valence and core) correlated and the Dunning's correlation consistent basis sets with polarized core-valence triple-ζ for explicitly correlated calculations (cc-pCVTZ-F12).[25,26] At the optimized geometry, electric dipole moment components along the *a*- and *b*-inertial axes were calculated at the same level of theory as that for the geometrical optimization. The calculations were performed using the MOLPRO 2020.2 program.[27] The fine and hyperfine coupling constants were estimated using the B3LYP[28] hybrid density functional with the augmented diffuse (aug-cc-pVTZ) basis set.[29] Harmonic and anharmonic vibrational frequencies were computed at the same level of theory to estimate the centrifugal distortion constants and the vibration-rotation interaction contribution to the rotational constants. These calculations were performed using the Gaussian16 program package.[30]

The rotational constants calculated by the optimized geometries (*xyz* coordinates at the Table SI of the ESI) with corrections for the vibration-rotation interactions are given in Tables 1 and 2 for the two species. The fine and hyperfine coupling constants are also given in these tables, which were used to initially assign the observed spectral patterns for observed rotational transitions.

RESULTS

α-ClVR. The predicted dipole moment components for α-ClVR are not so large, in particular the *b*-component (0.34D). Hence, we first tried to observe *a*-type rotational transitions (μ_a=0.80D). Following the transition frequency predictions using the theoretical data of Table 1, we observed a group of about fifty paramagnetic lines at 11.4 GHz frequency region. These lines were assigned to the $N_{Ka,Kc} = 1_{0,1}–0_{0,0}$ rotational transition after observing two other groups of lines at 22.7 and 34.0 GHz that correspond to $N_{Ka,Kc} = 2_{0,2}–1_{0,1}$ and $3_{0,3}–2_{0,2}$ transitions (see

Figure 2), respectively. In addition, we observed weaker lines at 22.4 and 23.0 GHz that are assigned as those belonging to the two K_a = 1 transitions, $N_{Ka,Kc}$ = $2_{1,2}$–$1_{1,1}$ and $2_{1,1}$–$1_{1,0}$, respectively. No attempts were made to measure any *b*-type rotational transitions, since they all fall out of the frequency range of the spectrometer, even for double resonance measurements.

All the observed rotational transition frequencies were analyzed using a reduced form of the Hamiltonian for doublet asymmetric top molecules[19,31] with C_s symmetry taking into account the fine and hyperfine interactions due to the three nuclear spins in the radical. The employed Hamiltonian has the following form:

$$H = H_{\mathrm{rot}} + H_{\mathrm{sr}} + H_{\mathrm{mhf}} + H_{\mathrm{Q}}$$

where H_{rot} contains rotational and centrifugal distortion parameters, H_{sr} is the spin–rotation interaction term, H_{mhf} represents the magnetic hyperfine interaction term due to the chlorine and two hydrogen nuclei, and finally H_{Q} represent the nuclear electric quadrupole interaction due to chlorine nucleus. The coupling scheme used in the present study is thus $\mathbf{J} = \mathbf{N} + \mathbf{S}$, $\mathbf{F_1} = \mathbf{J} + \mathbf{I}(\mathrm{Cl})$, $\mathbf{F_2} = \mathbf{F_1} + \mathbf{I}(\mathrm{H_1})$ and $\mathbf{F} = \mathbf{F_2} + \mathbf{I}(\mathrm{H_2})$, where **N** is the angular momentum of the molecular rotation, **S** is the electron spin angular momentum, and **I**(X) is the nuclear spin angular momentum of the chlorine and hydrogen nuclei.

The list of measured transitions for α-ClVR contains 207 hyperfine components from five rotational transitions. All the observed lines and their assignments are listed in Table SII of the ESI. Twenty-one molecular constants were determined by the least-squares analysis for all the observed transition frequencies. The standard deviation of the fit is 1.6 kHz, which is slightly smaller than the experimental accuracy of the measurements, indicating that the complicated hyperfine structures caused by the three coupling nuclei are well described by the employed Hamiltonian. The determined molecular constants are summarized in Table 1 along with those predicted by *ab initio* calculations.

Lines of ^{37}Cl isotopologue for α-ClVR were easily found after appropriately scaling the rotational constants using the observed molecular constants for ^{35}Cl and those obtained by *ab initio* calculations. The final dataset for the ^{37}Cl isotopologue consists of 110 hyperfine components (Table SIII of the ESI) from the three rotational transitions $N_{Ka,Kc}$ = $1_{0,1}$–$0_{0,0}$, $2_{0,2}$–$1_{0,1}$ and $3_{0,3}$–$2_{0,2}$. The K_a = 1 transitions could not be measured because they are too weak. The results derived from the spectral analysis are shown in Table 1.

β-ClVR. As mentioned before β-ClVR is predicted to have two isomers, *trans*-β-ClVR and *cis*-β-ClVR. We first searched for the spectral features of *trans*-β-ClVR, which is predicted to be more stable than *cis*-β-ClVR, and directly produced from *trans*-1,2-dichloroethylene. As the *a*-component of the dipole moment (0.93 D) is much larger than the *b*-component (0.06 D), we scanned the predicted frequency regions for *a*-type lines. Five *a*-type rotational transitions $N_{Ka,Kc}$ = $1_{0,1}$–$0_{0,0}$, $2_{1,2}$–$1_{1,1}$, $2_{0,2}$–$1_{0,1}$, $2_{1,1}$–$1_{1,0}$ and $3_{0,3}$–$2_{0,2}$ were observed by FTMW measurements (see Figure 2). In spite of the fact that *b*-type transitions are predicted to be extremely weak, we tried to observe the $N_{Ka,Kc}$ = $1_{1,0}$–$1_{0,1}$ transition by double resonance measurements (see Figure 3), and we were able to detect seven hyperfine components for that transition. Hence, a total of 342 hyperfine transitions (Table SIV of the ESI) were analyzed using the same Hamiltonian employed for α-ClVR with the standard deviation of the fit of 3.0 kHz. The molecular constants determined by the least-squares fittings together with those predicted theoretically are listed in Table 2. As has been done for α-ClVR, rotational transitions for the ^{37}Cl isotopologue of *trans*-β-ClVR were easily found after appropriately scaling the rotational constants using the observed molecular constants for ^{35}Cl and those of *ab initio* calculations. A total of 76 hyperfine components (Table SV of the ESI) were observed for the ^{37}Cl isotopologue and analyzed in the same manner than the other isotopologues. The results derived from the spectral analysis are shown in Table 2.

After assigning all the lines for the *trans*-β-ClVR isomer, we searched for the rotational transitions of the *cis*-β-ClVR isomer which is predicted to be ~5 kJ mol^{-1} less stable than the

trans isomer. However, we could not find any lines attributable to this species after scanning the predicted frequency regions.

DISCUSSION

The detection of the α-ClVR and *trans* isomer of β-ClVR and the non-observation of the *cis* isomer of β-ClVR can be accounted for the radical precursors employed in our experiments. 1,1-dichloroethylene and *trans*-1,2-dichloroethylene undergo a Cl abstraction in the electric discharge process. Both Cl atoms are equivalent in 1,1-dichloroethylene and *trans*-1,2-dichloroethylene, and thus they can only generate one product by abstraction of a Cl atom, α-ClVR and *trans*-β-ClVR, respectively. The generation of the *cis* isomer of β-ClVR would require the use of a different precursor.

As it can be seen in Tables 1 and 2, the agreement between the experimental and predicted values for the rotational constants of both α-ClVR and β-ClVR are very nice. The B_0 and C_0 theoretical constants show relative errors from the experimental values smaller than 0.05%, while the relative error for the A_0 constant, determined only for β-ClVR, is fairly large, around 0.4%. Similar results have been found in previous works using the same level of calculation.[32–36] On the other hand, the centrifugal distortion constants Δ_N and Δ_{NK} are reasonably well reproduced by the B3LYP/aug-cc-pVTZ theoretical calculations.

The electron spin-rotation constants calculated also at the B3LYP/aug-cc-pVTZ level of theory agree well with the experimental ones, better in the case of the α-ClVR, with the exception of ε_{ab} value, which shows large discrepancies between the theoretical and experimental values. We carried out also calculations at the MP2 level of theory and the results were also unsatisfactory for this constant. Several hyperfine constants were included in the fit for the Cl nucleus, including Fermi contact constant, dipole-dipole constants, nuclear quadrupole coupling constants and the nuclear spin-rotation constants. The experimental values for all of them, for both α-ClVR and *trans*-β-ClVR, are well reproduced by the B3LYP/aug-cc-pVTZ calculations. The agreement between the experimental and theoretical values for the same

constants of H nuclei are similar to those found for the Cl nucleus, with the exception of the Fermi contact constant of the H_1 nucleus for the *trans*-β-ClVR. The experimental value is 9.86837(71) MHz, while the theoretical one is 35.2 MHz. Other levels of theory also provide similar values for this Fermi contact constant. This discrepancy means the spin density on the H_1 nucleus for the *trans*-β-ClVR cannot be calculated well by these methods. Furthermore, this fact constituted the main reason why we found several difficulties to initially assign the rotational spectrum of the *trans*-β-ClVR.

As mentioned before, both α-ClVR and *trans*-β-ClVR have $^2A'$ electronic ground state and they are so called σ-radicals, in which the unpaired electron occupies an in plane molecular orbital. The unpaired electron orbitals for α-ClVR and *trans*-β-ClVR are shown in Figure 4. The experimental constants can be used to compare the spin properties for α-ClVR and *trans*-β-ClVR. All the electronic spin-rotation constants for α-ClVR are different to those for *trans*-β-ClVR, in sign and magnitude. This fact can be understood because of the difference in the directions of the principal axes in both radicals. The electronic spin-rotation constants ε_{aa} and ε_{cc} have negative values for α-ClVR while they are positive for *trans*-β-ClVR. The same behavior for ε_{aa} and ε_{cc} having negative values has been recently reported for the *cis*-β-cyanovinyl radical,[19] see Table 3. The reason why ε_{aa} is negative for α-ClVR is difficult to understand, because it is usually positive for σ-radicals. The contribution of excited electronic states to the spin-rotation interaction should be examined to understand why ε_{aa} is negative. However, it may not be so easy and is out of the scope of the present work. The Fermi contact terms of the chlorine atom show similar values in the two radicals while the values for the dipole-dipole coupling constants, T_{aa} and T_{bb}, are interchanged from α-ClVR to *trans*-β-ClVR, due to different orientations of the unpaired electron orbital extending from the chlorine atom in the two radicals, as can be seen in Figure 4. Fermi constants for the H nuclei are different in both radicals. Those for the α-ClVR are similar to those derived for vinyl radical[17] and, as mentioned before, agree reasonably well with those predicted theoretically.

CONCLUSIONS

Two isomers of chlorine derivatives of vinyl radical, α-ClVR and *trans*-β-ClVR, have been observed through their rotational spectra. They have been generated in an electric discharge using 1,1-dichloroethylene and *trans*-1,2-dichloroethylene, respectively, diluted in Ar. For both radicals ^{35}Cl and ^{37}Cl isotopologues were observed. The observed fine/hyperfine components of each rotational transition were successfully assigned, and the molecular parameters of the radicals were precisely determined for the first time. Experimental fine and hyperfine coupling constants for hydrogen nuclei are compared to those of analogue species like the vinyl radical and its cyano derivative, *cis*-β-cyanovinyl radical.

SUPPLEMENTARY MATERIAL

See supplementary material for the measured transition frequencies.

AUTHOR CONTRIBUTIONS

Carlos Cabezas. Data curation, Formal Analysis, Investigation, Project administration, Writing – original draft. **Ching-Hua Chang.** Formal Analysis, Investigation, Writing – review & editing. **Jean-Claude Guillemin.** Investigation, Writing – review & editing. **Yasuki Endo.** Conceptualization, Data curation, Formal Analysis, Funding acquisition, Methodology, Software, Writing – review & editing

CONFLICTS OF INTEREST

There are no conflicts to declare.

ORCID

Carlos Cabezas. https://orcid.org/0000−0002−1254−7738

Ching-Hua Chang. https://orcid.org/0000-0002-2008-8439

Jean-Claude Guillemin. https://orcid.org/0000-0002-2929-057X

Yasuki Endo. https://orcid.org/0000-0002-8660-6729

ACKNOWLEDGEMENTS

The present study was supported by the Ministry of Science and Technology of Taiwan, MOST 104-2113-M-009-202. JCG thanks the Centre National d'Etudes Spatiales (CNES) for a grant.

REFERENCES

1 J. A. Thornton, J. P. Kercher, T. P.Riedel, N. L.Wagner, J.Cozic, J. S.Holloway, W. P.Dub́, G. M.Wolfe, P. K.Quinn, A. M.Middlebrook, B.Alexander and S. S.Brown, A large atomic chlorine source inferred from mid-continental reactive nitrogen chemistry, *Nature*, 2010, **464**, 271–274.

2 C.-T.Chang, T.-H.Liu and F.-T.Jeng, Atmospheric concentrations of the Cl atom, CIO radical, and HO radical in the coastal marine boundary layer, *Environ. Res.*, 2004, **94**, 67–74.

3 T. H.Lowry andK. S.Richardson, *Mechanism and Theory in Organic Chemistry*, HarperCollins, New York, 1987.

4 C. A.Taatjes, Time-resolved infrared absorption measurements of product formation in Cl atom reactions with alkenes and alkynes, *Int. Rev. Phys. Chem.*, 1999, **18**, 419–458.

5 M. J.Molina, L. T.Molina and C. E.Kolb, Gas-phase and heterogeneous chemical kinetics of the troposphere and stratosphere, *Annu. Rev. Phys. Chem.*, 1996, **47**, 327–367.

6 E. W.Kaiser and T. J.Wallington, Kinetics of the Reactions of Chlorine Atoms with C_2H_4 (k_1) and C_2H_2 (k_2): a Determination of ΔH_f , 298° for C_2H_3, *J. Phys. Chem.* 1996, **4**, 4111–4119.

7 E. W.Kaiser, Pressure dependence of the reaction Cl + C_2H_2 over the temperature range 230 to 370 K, *Int. J. Chem. Kinet.*, 1992, **24**, 179–189.

8 T. J.Wallington, J. M.Andino, I. M.Lorkovic, E. W.Kaiser and G.Marston, Pressure dependence of the reaction of chlorine atoms with ethene and acetylene in air at 295 K, *J. Phys. Chem.*, 1990, **94**, 3644–3648.

9 T.Zhu, G.Yarwood, J.Chen and H.Niki, FTIR Study of the Cl + C_2H_2 Reaction: Formation of cis- and trans-CHCl:CH Radicals, *J. Phys. Chem.*, 1994, **98**, 5065–5067.

10 L.Zhu, W.Chen, W. L.Hase and E. W.Kaiser, Comparison of models for treating angular momentum in RRKM calculations with vibrator transition states: pressure and temperature dependence of chlorine atom + acetylene association, *J. Phys. Chem.*, 1993, **97**, 311–322.

11 J.Brunning and L. J.Stief, Pressure dependence of the absolute rate constant for the reaction Cl+ C_2H_2 from 210–361 K, *J. Chem. Phys.*, 1985, **83**, 1005–1009.

12 F. S. C.Lee and F. S.Rowland, The reaction of chlorine atoms with acetylene and its possible stratospheric significance, *J. Phys. Chem.*, 1977, **81**, 684–685.

13 S. M.Resende, J. R.Pliego Jr. and W. B.DeAlmeida, Free radical mechanism of the Cl_2 addition to acetylene, *J. Chem. Soc. Faraday Trans.*, 1998, **94**, 2895–2900.

14 J.-L.Li, C.-Y.Geng, X.-R.Huang, J.-H.Zhan and C.-C.Sun, F/Cl+ C_2H_2 reactions: Are the addition and hydrogen abstraction direct processes?, *Chem. Phys.*, 2006, **331**, 42–54.

15 L.Zhang, D. G.Truhlar and S.Sun, Association of Cl with C_2H_2 by unified variable-reaction-coordinate and reaction-path variational transition-state theory, *Proc. Natl. Acad. Sci. U. S. A.*, 2020, **117**, 5610–5616.

16 Y.Gao, I. M.Alecu, P. C.Hsieh, A.McLeod, C.McLeod, M.Jones and P.Marshall,

Kinetics and thermochemistry of the addition of atomic chlorine to acetylene, *Proc. Combust. Inst.*, 2007, **31 I**, 193–200.

17 K.Tanaka, M.Toshimitsu, K.Harada and T.Tanaka, Determination of the proton tunneling splitting of the vinyl radical in the ground state by millimeter-wave spectroscopy combined with supersonic jet expansion and ultraviolet photolysis, *J. Chem. Phys.*, 2004, **120**, 3604–3618.

18 S. L.Johansen, M.-A.Martin-Drumel and K. N.Crabtree, Rotational Spectrum of the β-Cyanovinyl Radical: A Possible Astrophysical N-Heterocycle Precursor, *J. Phys. Chem. A*, 2019, **123**, 5171–5177.

19 M.Nakajima, Y.-T.Liu, C. H.Chang, K.Seiki, Y.Sumiyoshi, Y.Ohshima, J.Tang and Y.Endo, Fine and hyperfine coupling constants of the cis -β-cyanovinyl radical, HCCHCN, *Phys. Chem. Chem. Phys.*, 2022, **24**, 11585-11591.

20 Y.Endo, H.Kohguchi and Y.Ohshima, PDN–FTMW spectroscopy of open-shell complexes, *Faraday Discuss.*, 1994, **97**, 341–350.

21 C.Cabezas, J.-C.Guillemin and Y.Endo, Fourier-transform microwave spectroscopy of a halogen substituted Criegee intermediate ClCHOO, *J. Chem. Phys.*, 2016, **145**, 184304.

22 Y.Sumiyoshi, H.Katsunuma, K.Suma and Y.Endo, Spectroscopy of Ar–SH and Ar–SD. I. Observation of rotation-vibration transitions of a van der Waals mode by double-resonance spectroscopy, *J. Chem. Phys.*, 2005, **123**, 054324.

23 T. B.Adler, G.Knizia and H.-J.Werner, A simple and efficient CCSD(T)-F12 approximation, *J. Chem. Phys.*, 2007, **127**, 221106.

24 G.Knizia, T. B.Adler and H.-J.Werner, Simplified CCSD(T)-F12 methods: Theory and benchmarks, *J. Chem. Phys.*, 2009, **130**, 054104.

25 J. G.Hill and K. A.Peterson, Correlation consistent basis sets for explicitly correlated wavefunctions: valence and core–valence basis sets for Li, Be, Na, and Mg, *Phys. Chem. Chem. Phys.*, 2010, **12**, 10460.

26 J. G.Hill, S.Mazumder and K. A.Peterson, Correlation consistent basis sets for molecular core-valence effects with explicitly correlated wave functions: The atoms B–Ne and Al–Ar, *J. Chem. Phys.*, 2010, **132**, 054108.

27 H.–J.Werner, P.J.Knowles, G.Knizia, F.R.Manby, M.Schütz, P.Celani, W.Györffy, D.Kats, T.Korona, R.Lindh, A.Mitrushenkov, G.Rauhut, K.R.Shamasundar, T.B.Adler, R.D.Amos, S.J.Bennie, A.Bernhardsson, A.Berning, D.L.Cooper, M.J.O.Deegan, A.J.Dobbyn, F.Eckert, E.Goll, C.Hampel, A.Hesselmann, G.Hetzer, T.Hrenar, G.Jansen, C.Köppl, S.J.R.Lee, Y.Liu, A.W.Lloyd, Q.Ma, R.A.Mata, A.J.May, S.J.McNicholas, W.Meyer, T.F.Miller III, M.E.Mura, A.Nicklass, D.P.O'Neill, P.Palmieri, D.Peng, K.Pflüger, R.Pitzer, M.Reiher, T.Shiozaki, H.Stoll, A.J.Stone, R.Tarroni, T.Thorsteinsson, M.Wang, M.Welborn, MOLPRO, version 2019.2, a package of ab initio programs, (2019).

28 A. D.Becke, A new mixing of Hartree–Fock and local density-functional theories, *J. Chem. Phys.*, 1993, **98**, 1372–1377.

29 D. E.Woon andT. H.Dunning, Gaussian basis sets for use in correlated molecular calculations. V. Core-valence basis sets for boron through neon, *J. Chem. Phys.*, 1995,

103, 4572–4585.

30 M. J.Frisch, G. W.Trucks, H. B.Schlegel, G. E.Scuseria, M. a.Robb, J. R.Cheeseman, G.Scalmani, V.Barone, G. a.Petersson, H.Nakatsuji, X.Li, M.Caricato, a.V.Marenich, J.Bloino, B. G.Janesko, R.Gomperts, B.Mennucci, H. P.Hratchian, J.V.Ortiz, a. F.Izmaylov, J. L.Sonnenberg, Williams, F.Ding, F.Lipparini, F.Egidi, J.Goings, B.Peng, A.Petrone, T.Henderson, D.Ranasinghe, V. G.Zakrzewski, J.Gao, N.Rega, G.Zheng, W.Liang, M.Hada, M.Ehara, K.Toyota, R.Fukuda, J.Hasegawa, M.Ishida, T.Nakajima, Y.Honda, O.Kitao, H.Nakai, T.Vreven, K.Throssell, J. a.Montgomery Jr., J. E.Peralta, F.Ogliaro, M. J.Bearpark, J. J.Heyd, E. N.Brothers, K. N.Kudin, V. N.Staroverov, T. a.Keith, R.Kobayashi, J.Normand, K.Raghavachari, a. P.Rendell, J. C.Burant, S. S.Iyengar, J.Tomasi, M.Cossi, J. M.Millam, M.Klene, C.Adamo, R.Cammi, J. W.Ochterski, R. L.Martin, K.Morokuma, O.Farkas, J. B.Foresman and D. J.Fox, 2016, Gaussian 16, Revision C.01, Gaussian, Inc., Wallin.

31 J. M.Brown and T. J.Sears, A reduced form of the spin-rotation Hamiltonian for asymmetric-top molecules, with applications to HO_2 and NH_2, *J. Mol. Spectrosc.*, 1979, **75**, 111–133.

32 J. Cernicharo, N. Marcelino, M. Agúndez, Y. Endo, C. Cabezas, C. Bermúdez, B. Tercero and P. deVicente, Discovery of HC_3O^+ in space: The chemistry of O-bearing species in TMC-1, *Astron. Astrophys.*, 2020, **642**, L17.

33 J. Cernicharo, C. Cabezas, Y. Endo, N. Marcelino, M. Agúndez, B. Tercero, J. D. Gallego and P. de Vicente, Space and laboratory discovery of HC_3S^+, *Astron. Astrophys.*, 2021, **646**, L3.

34 J. R. Pardo, C. Cabezas, J. P. Fonfría, M. Agúndez, B. Tercero, P.de Vicente, M. Guélin and J. Cernicharo, Magnesium radicals MgC_5N and MgC_6H in IRC+10216, *Astron. Astrophys.*, 2021, **652**, L13.

35 C. Cabezas, M. Agúndez, N. Marcelino, B. Tercero, Y. Endo, R. Fuentetaja, J. R. Pardo, P. de Vicente and J. Cernicharo, *Astron. Astrophys.*, 2022, **657**, L4.

36 M. Agúndez, C. Cabezas, N. Marcelino, R. Fuentetaja, B. Tercero, P. de Vicente and J. Cernicharo, *Astron. Astrophys.*, 2022, **659**, L9.

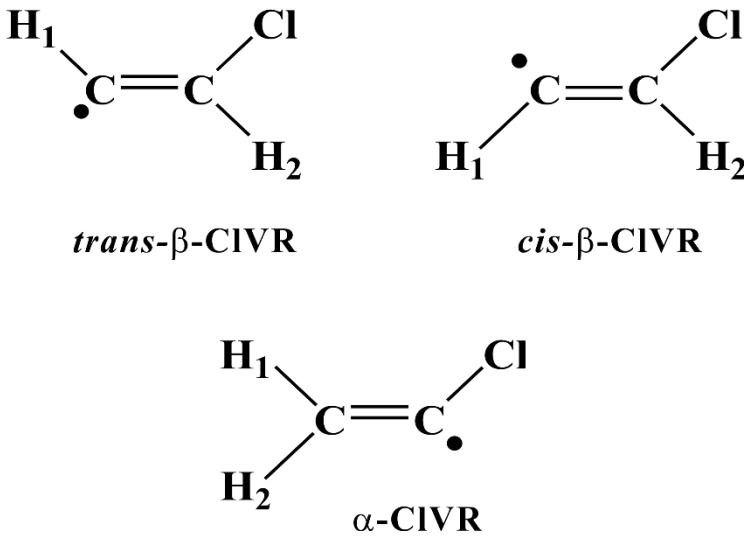

Figure 1. The three isomers of the chlorovinyl radical.

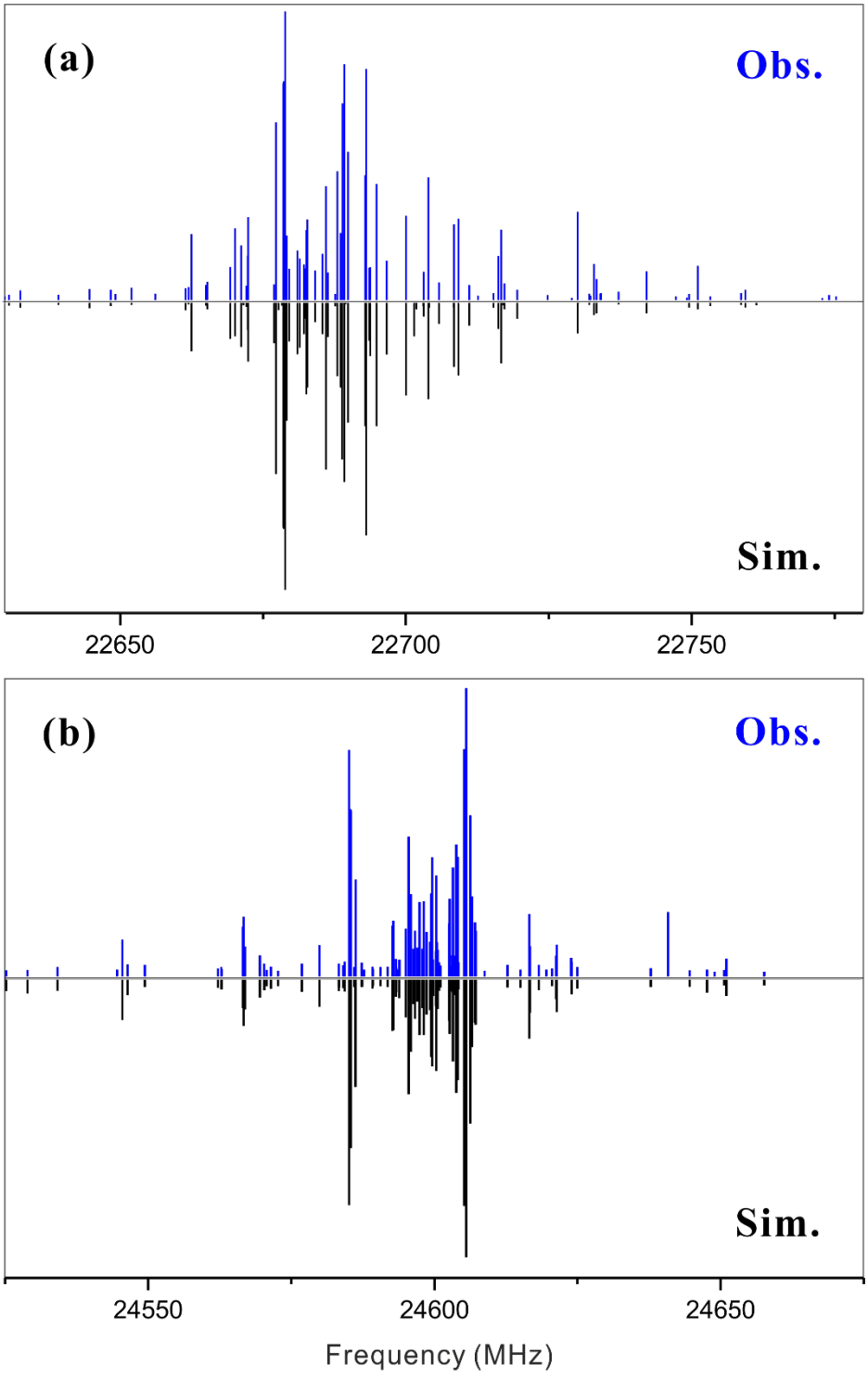

Figure 2. Line intensities for the $2_{0,2}$–$1_{0,1}$ rotational transition of α-ClVR (a) and *trans*-β-ClVR (b) observed using FTMW spectroscopy (blue sticks). The sticks inverted below are simulations using the determined molecular constants in Tables 1 and 2.

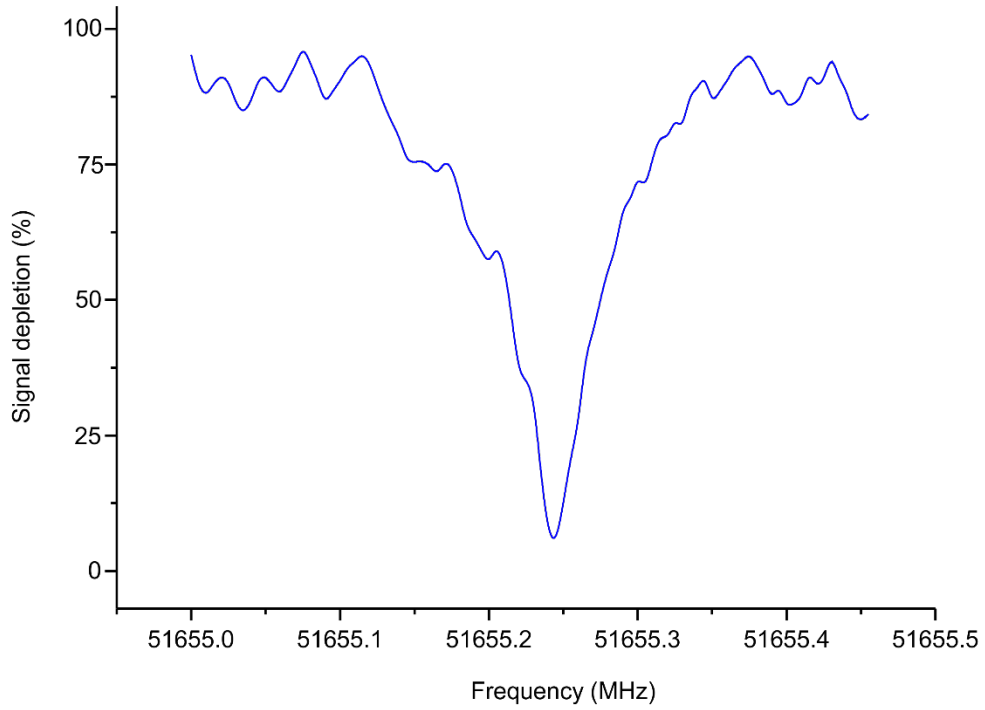

Figure 3. FTMW–MW double-resonance spectrum of one hyperfine component of the $1_{1,0}$–$1_{0,1}$ transition of *trans*-β-ClVR at 51655.269 MHz, observed by monitoring the 25281.319 MHz line of the $2_{1,1}$–$1_{1,0}$ transition.

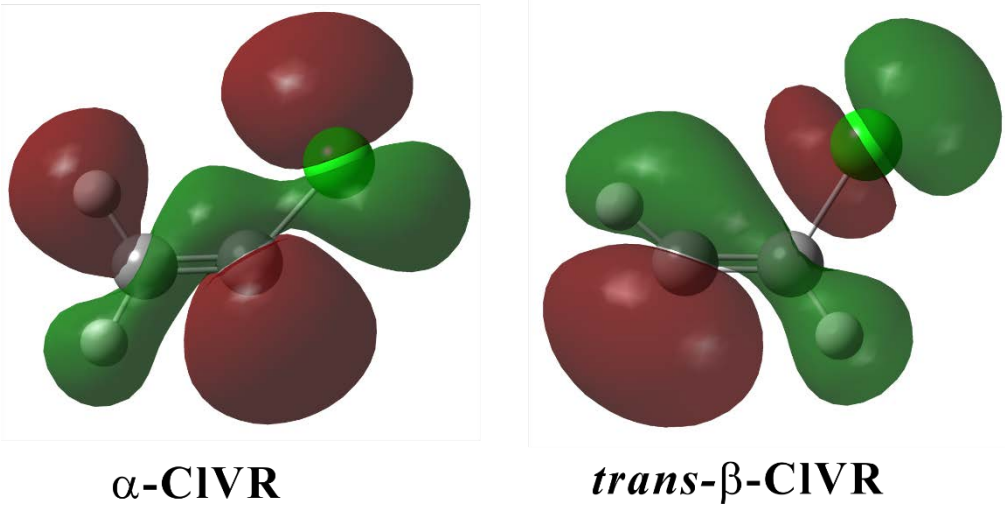

Figure 4. The unpaired electron orbital of α-ClVR and *trans*-β-ClVR in their $^2A'$ ground electronic states calculated at the RCCSD(T)-F12A;core/cc-pCVTZ-F12 level of theory. The colors of the orbital lobes reflect the phases of the orbital.

Table 1. Molecular constants of α-ClVR (all in MHz).

	α-ClVR ^{35}Cl		α-ClVR ^{37}Cl	
	Experimental	Theory[a]	Experimental	Theory[a]
A_0	109854[b]	109854	109693	109693
B_0	5823.51349(18)[c]	5821	-	-
C_0	5521.09343(18)	5521	-	-
$(B_0+ C_0)/2$			5559.86135(17)	5559
B_0-C_0			219	219
Δ_N	0.0030051(51)	0.00275	0.002886(12)	0.00275
Δ_{NK}	-0.166125(91)	-0.158	[-0.166125][d]	-0.158
ε_{aa}	-232.0987(21)	-204.8	[-232.0987]	-204.8
ε_{bb}	6.3090(16)	9.5	6.26(19)	9.5
ε_{cc}	-54.2179(16)	-57.3	-53.23(18)	-57.3
ε_{ab}	$\pm$4.5(1.3)[e]	-108.1	[$\pm$4.5]	-108.1
$a_F^{(Cl)}$	40.03396(39)	42.5	33.3442(13)	35.3
$T_{aa}^{(Cl)}$	-24.03391(51)	-26.0	-19.9509(12)	-21.6
$T_{bb}^{(Cl)}$	47.1682(20)	50.3	40.35(38)	41.8
$T_{ab}^{(Cl)}$	$\mp$26.6[e]	-26.6	$\mp$22.3[e]	-22.3
$\chi_{aa}^{(Cl)}$	-55.6707(15)	-51.0	-43.9386(34)	-40.2
$\chi_{bb}^{(Cl)}$	19.1016(56)	16.8	13.3	13.3
$\chi_{ab}^{(Cl)}$	30.3	30.3	23.8	23.8
$C_{aa}^{(Cl)}$	0.0278(11)	0.0309	[0.0278]	0.0257
$C_{bb}^{(Cl)}$	0.00392(21)	0.0019	[0.0039]	0.0016
$a_F^{(H1)}$	131.5399(27)	121.9	131.547(13)	121.9
$T_{aa}^{(H1)}$	1.9983(17)	2.4	1.9850(44)	2.4
$T_{bb}^{(H1)}$	2.9588(40)	3.1	[2.9588]	3.1
$T_{ab}^{(H1)}$	$\pm$3.6[e]	3.6	$\pm$3.6[e]	3.6
$a_F^{(H2)}$	57.7749(11)	54.4	57.7766(39)	54.4
$T_{aa}^{(H2)}$	11.8292(16)	12.2	11.8205(41)	12.2
$T_{bb}^{(H2)}$	-5.1276(50)	-5.2	[-5.1276]	-5.2
$T_{ab}^{(H2)}$	$\pm$4.5[e]	4.5	$\pm$4.5[e]	4.5

[a] RCCSD(T)-F12A;core/cc-pCVTZ-F12 for the A_0, B_0 and C_0 rotational constants and B3LYP/aug-cc-pVTZ for the rest of molecular constants. [b] Values without uncertainties have been kept fixed to those obtained theoretically. [c] Values in parentheses denote 1σ errors, applied to the last digit. [d] Values in brackets have been kept fixed to those experimentally determined for the ^{35}Cl isotopologue theoretically. [e] Only the relative signs are determined.

Table 2. Molecular constants of β-ClVR (all in MHz).

	trans-β-ClVR ^{35}Cl		*trans*-β-ClVR ^{37}Cl		*cis*-β-ClVR
	Experimental	Theory[a]	Experimental	Theory[a]	Theory[a]
A_0	57457.5039(13)[b]	57692	57361[c]	57361	74180
B_0	6483.86279(30)	6486	6347.96649(72)	6348	6198
C_0	5816.07623(31)	5820	5705.51922(74)	5708	5711
Δ_N	0.004992(11)	0.004976	0.004716(63)	0.004976	0.00349
Δ_{NK}	-0.08963(19)	-0.08542	-0.08675(30)	-0.08542	-0.105
ε_{aa}	35.2245(17)	51.0	34.2887(98)	51.0	174.2
ε_{bb}	44.0285(18)	54.6	43.2214(41)	54.6	15.8
ε_{cc}	12.9692(13)	12.6	12.7355(45)	12.6	25.2
ε_{ab}	±38.83(32)[d]	219.5	±38.83(32)[d]	219.5	386.3
$a_F^{(Cl)}$	42.43429(44)	34.6	35.3397(18)	34.6	27.3
$T_{aa}^{(Cl)}$	47.35339(82)	45.3	39.4141(17)	37.7	26.6
$T_{bb}^{(Cl)}$	-22.0619(12)	-20.6	-18.355(6)	-17.1	-10.7
$T_{ab}^{(Cl)}$	∓2.87(26)[d]	-0.4	∓2.19[e]	-0.2	-3.9
$\chi_{aa}^{(Cl)}$	-61.5430(15)	-59.0	-48.6212(37)	-46.6	-59.0
$\chi_{bb}^{(Cl)}$	27.0447(22)	27.0	21.422(23)	21.4	27.0
$\chi_{ab}^{(Cl)}$	34.9(11)	32.3	25.2	25.2	32.3
$C_{aa}^{(Cl)}$	0.00655(59)	0.0080	[0.00655][f]	0.007	0.0092
$C_{bb}^{(Cl)}$	0.0017317(21)	0.0016	[0.0017317]	0.0013	0.0021
$C_{cc}^{(Cl)}$	0.0017	0.0017	0.0014	0.0014	0.0016
$a_F^{(H1)}$	9.86837(71)	35.2	9.8749(26)	35.2	11.0
$T_{aa}^{(H1)}$	-0.8417(25)	-4.2	-0.8962(52)	-4.2	39.9
$T_{bb}^{(H1)}$	31.8966(33)	37.2	31.950(13)	37.2	-5.7
$T_{ab}^{(H1)}$	±12.57(60)[d]	12.3	±12.57	12.3	2.7
$C_{aa}^{(H1)}$	-0.00215(81)	-0.0053	[-0.00215]	-0.0053	0.014
$C_{bb}^{(H1)}$	0.00083(34)	0.0011	[0.00083]	0.0011	-0.0006
$C_{cc}^{(H1)}$	-0.0007	-0.0007	-0.0007	-0.0007	-0.0006
$a_F^{(H2)}$	64.37369(91)	60.5	64.3760(51)	60.5	123.7
$T_{aa}^{(H2)}$	3.0540(23)	3.4	3.0203(51)	3.4	2.1
$T_{bb}^{(H2)}$	2.7230(41)	2.8	2.769(19)	2.8	3.9
$T_{ab}^{(H2)}$	±6.24(68)[d]	7.6	±6.24	7.6	2.6
$C_{aa}^{(H2)}$	-0.00324(48)	-0.0061	[-0.00324]	-0.0061	-0.0074
$C_{bb}^{(H2)}$	0.00185(48)	0.0007	[0.00185]	0.0007	0.0006
$C_{cc}^{(H2)}$	-0.0006	-0.0006	-0.0006	-0.0006	-0.0005

[a] RCCSD(T)-F12A;core/cc-pCVTZ-F12 for the A_0, B_0 and C_0 rotational constants and B3LYP/aug-cc-pVTZ for the rest of molecular constants. [b] Values in parentheses denote 1σ errors, applied to the last digit. [c] Values without uncertainties have been kept fixed to those obtained theoretically. [d] Only the relative signs are determined. [e] Calculated using the experimental/theoretical value factor of the ^{35}Cl isotopologue. [f] Values in brackets have been kept fixed to those experimentally determined for the ^{35}Cl isotopologue theoretically.

Table 3. Fine and hyperfine constants of ClVRs and other vinyl radicals. (all in MHz).

	trans-β-ClVR	α-ClVR	*cis*-β-Cyanovinyl	Vinyl[a]
ε_{aa}	35.2245(17)[b]	-232.0987(21)	-6.624	232.401
ε_{bb}	44.0285(18)	6.3090(16)	3.380	2.9795
ε_{cc}	12.9692(13)	-54.2179(16)	-5.897	-35.9788
$a_F^{(H1)}$	9.86837(71)	131.5399(27)	96.5	143.353
$a_F^{(H2)}$	64.37369(91)	57.7749(11)	31.63	37.0192

[a] Average value (or calculated from the average values) between the 0^+ and 0^- sublevels, reported by Tanaka et al.[17] [b] Values in parentheses denote 1σ errors, applied to the last digit.